Determination of GaAs MESFETs self heating temperature via output conductance frequency dispersion

Z. HADJOUB, F. Z. KHELIFATI, D. NEBTI, A. GUERAOUI, A. DOGHMANE*
Laboratoire des Semi-Conducteurs, Département de Physique, Faculté des Sciences, Université Badji-Mokhtar, BP 12, Annaba, DZ-23000, Algérie.

In this paper, the output conductance frequency dispersion, $g_{d,}$ of GaAs MESFET is measured and analyzed in a large frequency range [10 Hz - 10^5 Hz]. The investigation was carried in the saturation regime for constant drain-source voltage, V_{ds} = 1 V, and at different negative values of gate-source voltage (- 0.6 V ≤ V_{gs} ≤ - 0.2 V). Moreover, a theoretical study of the frequency dispersion of g_d was carried out under the same experimental conditions. From the comparison between theoretical and experimental results we were able to determine the self heating temperature of the operated device at different gate-source voltages. It was found that this temperature decreases linearly with increasing $|V_{gs}|$ for which an analytical formula of the form $T(K) = T_0 - \beta V_{gs}$ was determined.

(Received March 18, 2013; accepted September 18, 2013)

Keywords: GaAs MESFET, output conductance, frequency dispersion, self heating.

1. Introduction

The good control of field effect transistor technology created an important impact in microwave devices. Great interest is shown, all over the world, in GaAs Metal Semiconductor Field Effect Transistors, MESFET, due to their multiple applications, in particular for ultra high speed logic circuits [1]. However, the performances of these devices present some anomalies at low frequencies, such as output conductance frequency dispersion and transconductance and hysteresis in current/voltage, I(V), characteristics [2-4]. These disadvantages have limited the design of integrated circuits and presented a serious problem for several applications in analog and digital circuits [5, 6]. The origin of these anomalies was attributed to the presence of traps in such devices [4, 7-9]. However, their location at the surface or in the channel-substrate interface is still a subject of research controversy and multiple discussions. Otherwise, the thermal effects in transistors induce slow dynamic variations.

Let's recall that the thermal state of a device results from transistor self-heating that is put into evidence by power dissipation. Moreover, the MESFET is a non-polar semiconductor device; the fundamental effect of heat creation is mainly associated with the Joule effect. This self-heating process may lead to a temperature gradient larger than 100 °C between the channel and the substrate [10]. In fact, when drain-source voltage increases, there is more power dissipated in the channel that makes it hotter.

In this work, we present a comparative study of theoretical and experimental results of the output conductance frequency dispersion $g_d(f)$ in GaAs MESFETs of commercial type. The agreement between theory and experiment allows the determination of the operating device temperature, T, of the device at a given voltage. Such a temperature, due to device self-heating, is a very important factor in the high power and high temperature applications. Thus, this approach to deduce T is carried out over a large frequency range [10 Hz -10^5 Hz] at several applied voltages.

2. Methodology

2.1 Principle

The adopted principle consists of optimizing of experimental results using calculated values in order to determine operating temperature. In the present theoretical simulations, we made use of output conductance expression proposed by Canfield et al. [6].

$$g_d(f) = \frac{g_d(lf)\left\{1 + j\,2\pi f\left(\tau_e \frac{g_d(hf)}{g_d(lf)}\right)\right\}}{(1 + j\,2\pi f\,\tau_e)} \qquad (1)$$

where g_d(lf) and g_d(hf) are the output conductance at low and high frequency, respectively; τ_e is the time constant for electron emission from mid-gap traps; it depends on the device characteristic frequency, f_c, and the operating temperature, T, [11, 12] as follows :

$$\tau_e = \frac{1}{f_c} \qquad (2)$$

with:

$$f_c = \frac{\sigma v_{th} N_c}{g} e^{-E_a/kT} \qquad (3a)$$

$$f_c = A T^2 e^{-E_a/kT} \qquad (3b)$$

where A is a constant that essentially depends on carriers effective mass, k is Boltzmann constant, σ is the capture cross section, T is the temperature of the device, v_{th} is the mean thermal velocity, N_c is the effective density of states in the conduction band, g is the level degeneracy factor (here, assumed as g = 1), and E_a is the activation energy.
It should be noted that for trap levels located in the gap of GaAs, the time constant for electron emissions related to device temperature, T, by the following relation [13]:

$$\tau_e \approx \frac{3.5\times10^{-8}}{T}\exp\left(\frac{9450}{T}\right) \quad (4)$$

Equations (1) and (4) shows that output conductance dependents on both frequency and temperature. It is a complex number that admits a modulus and a phase.

Experimentally, we measure the modulus of the output conductance. Hence, in order to compare experimental and simulated results, it is necessary to determine the modulus of the expression (1). Moreover, to facilitate the calculations and comparison, we adopted, in this work, relative values. Thus, the value of the output conductance is normalized to that obtained at the lowest frequency, g_d(lf). Finally, the relation used in the calculations of g_d(f) in the whole frequency range is given by:

$$\left|\frac{g_d(f)}{g_d(lf)}\right| = \sqrt{\frac{1+4\pi^2 f^2\left(\tau_e \frac{g_d(hf)}{g_d(lf)}\right)^2}{1+4\pi^2 f^2 \tau_e^2}} \quad (5)$$

In this investigation, the first measurement frequency is 10 Hz at which the output conductance, g_d(lf), is first calculated. Then, using Eqn. 5, we determine $g_d(f)/g_d(lf)$. Finally, the temperature of the transistor is obtained from the best agreement obtained when experimental and calculated results are compared.

2.2 Calculating steps

The calculation steps are summarized in Fig. 1; they consist of:

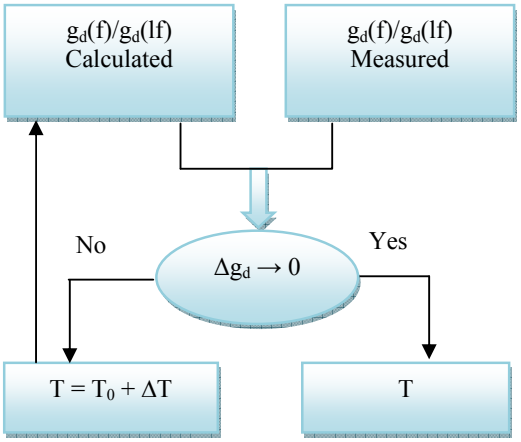

Fig. 1. Diagram of the simulation steps.

✓ Estimating, at room temperature, the output conductance frequency dispersion in the frequency range used for the measurement.
✓ Determining the discrepancy, Δg_d, between calculated results and those determined experimentally, as defined by:

$$\Delta g_d = \|[g_d(f)/g_d(lf)_{cal.}]-[g_d(f)/g_d(lf)_{meas.}]\| \quad (6)$$

✓ Analyzing the discrepancy: if Δg_d approaches zero, the deduced temperature is the operating temperature of the device. Otherwise, we increase the temperature and repeat the procedure until Δg_d approaches a null value.

3. Results and discussion

3.1. Observation of theory-experiment discrepancy

We first measure experimentally and calculate theoretically, at room temperature, the output conductance frequency dispersion. The obtained results, at V_{gs} = - 0.3 V, are plotted in Fig. 2 in terms of output conductance, normalized to the lowest used frequency (lf = 10 Hz), as a function of frequency for experimental data, (▪) and theoretical simulations (——) .

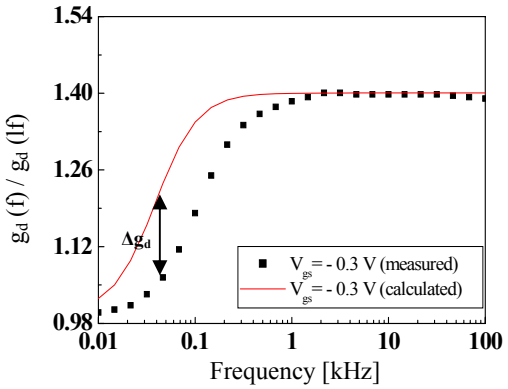

Fig. 2. $|g_d(f)/g_d(lf)|$variations with frequency obtained, at 300 K, experimentally (▪) and theoretically (——) for V_{gs} = - 0.3 V

It can clearly be seen that the calculated values of $g_d(f)/g_d(lf)$ are larger than those measured under the same conditions. The discrepancy, Δg_d, obtained at room temperature, is clearly indicated by an arrow. It is worth noting that similar behaviors, as above, were also obtained for other gate-source voltages (- 0.2 V; - 0.35 V; - 0.4 V, 0.45 V and – 0.6 V).

3.2. Effects of temperature and frequency

The effects of temperature and frequency on output conductance are illustrated in Fig. 3 in terms of $|g_d(f)/g_d(lf)|$ as a function of frequency obtained experimentally (▪) and theoretically (——) at V_{ds}= 1 V et

V_{gs}= - 0.2 V and different temperatures. It is clear that the output conductance exhibits positive dispersion for lower frequencies (f ≤ 4 10^3 Hz). Whereas, for higher frequencies (f > 4 10^3 Hz), the output conductance values becomes almost constant and independent of changes in the frequency.

A close look and a rigorous analysis of these curves shows that the best theory-experiment agreement is obtained for T = 327 K (Fig. 3 b) However, as the temperature departs from this value, the discrepancy between theory-experiment becomes more important.

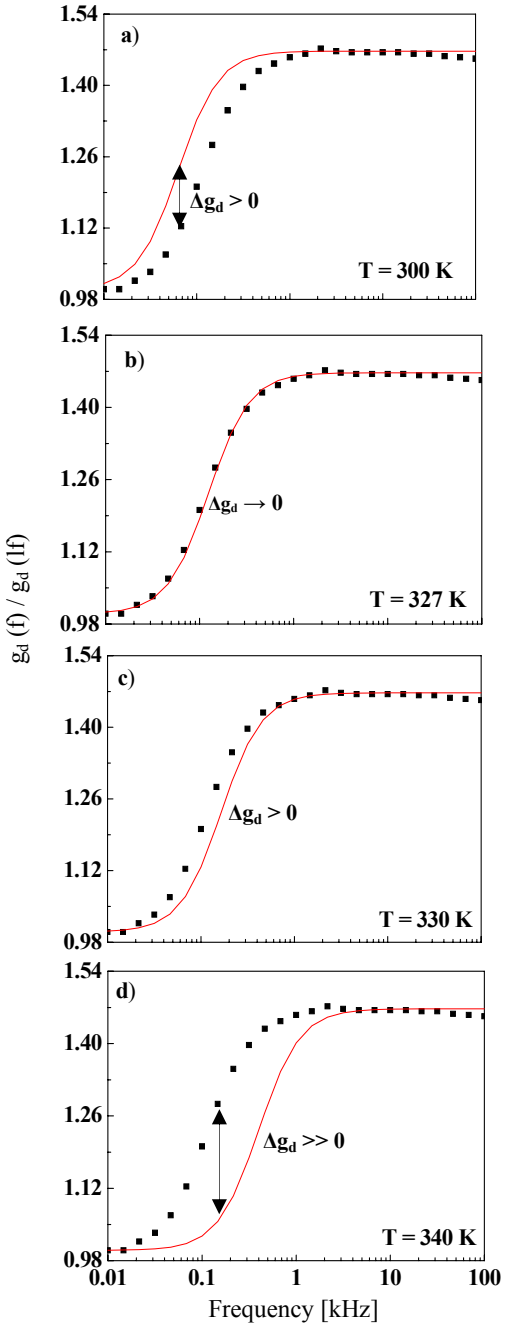

Fig. 3. $|g_d(f)/g_d(lf)|$ variations with frequency: theory (—) and experiment (▪) at V_{gs}=-0.2V and V_{ds}= 1V.

For higher temperatures (T > 327 K), the discrepancy reappears with experimental results being higher than those calculated (Fig. 3c and Fig. 3d). For T < 327 K, the calculated values are higher than those measured experimentally (Fig. 3a). Thus, for bias conditions defined by V_{ds} = 1 V and V_{gs}= - 0.2 V, the transistor operating temperature would be 327 K meaning that the self heating of the device caused an increase of 27 K higher than room temperature at which the MESFET it is used.

In order to better illustrate the effects of temperature and frequency on Δg_d, we plot in Fig. 4 typical results, obtained at V_{ds} = 1 V and V_{gs} = - 0.2 V, of Δg_d (Eq. 6), as a function of temperature for different frequency values (f = 10, 20, 100, 10^3 and 10^4 Hz). Several behaviors can be observed according to temperature and/or frequency values:

a) For f ≥ 10^3 Hz, Δg_d is nearly constant throughout the temperature range and its value is practically zero.

b) For f < 10^3 Hz, we observe two opposite behaviors: (i) Δg_d decreases down to a null value when the temperature increases up to 327K and (ii) beyond 327 K, Δg_d increases up to 20% when T reaches 340 K.

c) At room temperatures, Δg_d generally decreases with increasing frequency.

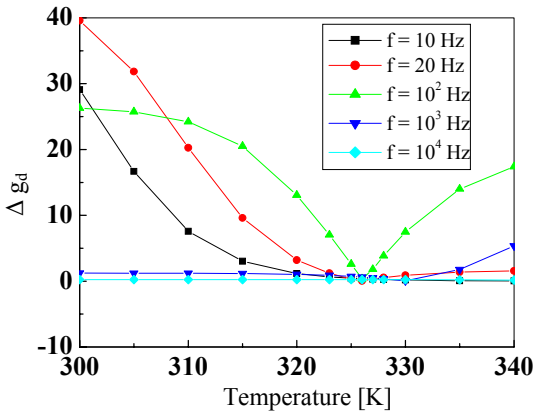

Fig. 4. Variations of $\Delta g_d = f(T)$ at different frequencies for V_{ds} = 1 V and V_{gs} = -0.2 V.

To put into evidence such behaviors, we consider the same investigation for other values of V_{gs} (- 0.3, - 0.35, - 0.4, - 0.45 and - 0.6 V). Indeed, similar curves as those shown in figures 3 and 4 where obtained. Thus, we can conclude that the effects of temperature can be neglected at high frequencies for f ≥ 10^3 Hz. This would confirm the fact that: (i) the existence of surface states is responsible for frequency dispersion and (ii) the traps cannot follow rapid signals when high frequencies are used.

3.3. Bias effects on operating temperature

It is worth noting that the output conductance variations of GaAs MESFET as a function of frequency and temperature are strongly influenced by bias conditions. These phenomena lead to several difficulties in device operation and in its applications in integrated

circuits. Hence, to put into evidence and to quantify this effect, we carry out this investigation at variable temperatures from 300 K to 340 K, at a constant V_{ds} = 1 V, in the frequency range [10 - 10^5 Hz] and with different gate-source voltages, V_{gs}, equal to: - 0.2 V, - 0.3 V, - 0.35 V, - 0.4 V, - 0.45 V and - 0.6 V.

In Table 1, we regroup some representative experimental values of g_d at low frequencies (f = 10 Hz) and high frequencies (f = 10^3 Hz) obtained for the previously chosen values of applied voltages. It can clearly be seen that, for all gate voltages the value of g_d at low frequency remains less than g_d at high frequencies, in all cases. However, when $|V_{gs}|$ increases the output conductance decreases in the whole range of frequencies.

Table 1. Experimental values of $g_d]_{10\ Hz}$ and $g_d]_{1kHz}$ obtained at V_{ds}=1 V and different values of V_{gs}.

$-V_{gs}$ (V)	$g_d]_{10\ Hz}$ (mS)	$g_d]_{1\ kHz}$ (mS)
0.20	4.13	6.06
0.30	3.92	5.49
0.35	3.37	4.85
0.40	2.98	4.24
0.45	2.41	3.44
0.60	0.79	1.13

To put into evidence the reproducibility of the previous results, we considered several $|V_{gs}|$ values (0.2 V, 0.30 V, 0.35 V, 0.40 V, 0.45 and 0.60 V). The obtained curves showed similar behaviors, experimentally and theoretically, as those previously found in Fig. 3 with discrepancies between theory and experiment except at a given specific temperature for each gate-source voltage.
The curves of best theory-experiment agreement obtained for different V_{gs} (0.2 V, 0.35 V, 0.45 V) are plotted in Fig. 5 in terms of $|g_d(f)/g_d(lf)|$ as a function frequency: theory (solid lines) and experiments (▪ ▲ ●). Differences in T are indicative of differences in operating device temperature for each indicated V_{gs}.

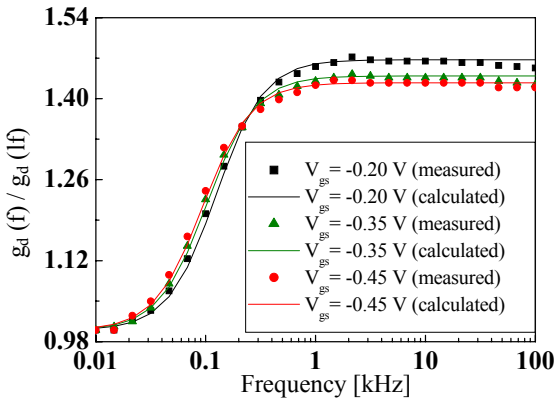

Fig. 5. $|g_d(f)/g_d(lf)|$ variations with frequency theory and experiment at V_{gs} = - 0.2 V, - 0.35 V and – 0.45 V for V_{ds} = 1 V

It can be seen that T decreases as $|V_{gs}|$ increases. This effect is better illustrated in Fig. 6 in terms of T versus $|V_{gs}|$. Using simple curve fitting, we were able to deduce a relation of the temperature dependence on gate-source voltage follows:

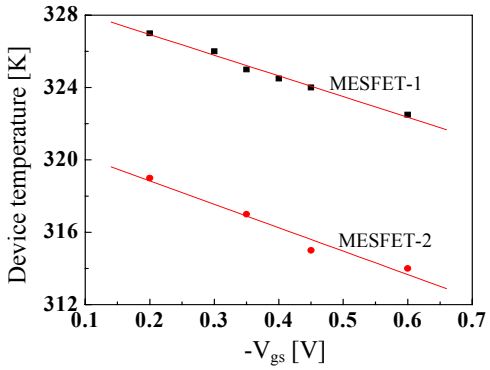

$$T(K) = 329 - 11.40\ V_{gs} \quad (7)$$

Fig. 6. Device temperature variations with gate-source voltage, for two MESFET types at V_{ds}=1 V

To confirm the reproducibility all the above obtained results, we carried out the same investigations on another type of commercial GaAs MESFETs. Similar results to those of the first MESFET were also obtained for (i) $g_d(f)$ curve behaviors (i.e., dispersion followed by constancy) and (ii) temperatures at which the theory-experiment agreements occur. The analysis and treatment of all the obtained results of the second GaAs MESFET led to a similar dependence of de device temperature on gate-source voltage. This dependence is better illustrated in Fig. 6 (lower curve). The relation between T and V_{gs} was also deduced and found to be of the form:

$$T\ (K) = 321 - 12.94\ V_{gs} \quad (8)$$

Thus, Eq. (7) and Eq. (8) can be generalized to other GaAs MESFETs that can be written as:

$$T(K) = T_0 - \beta V_{gs} \quad (9)$$

where T_0 is the characteristic temperature at V_{gs} = 0 V and β is the slope of the curve $T = f(V_{gs})$.

It should be noted that, at constant V_{ds}, any increase in $|V_{gs}|$ leads to an expansion of the depletion region. Therefore, the conductive channel gets narrower and consequently the density of free carriers crossing the active zone decreases causing a decrease in drain current. This heating phenomenon appears in the channel region as a result of drain current flux and consequently to power dissipation. The major heat quantity is produced between the gate and the drain side since this region supports the majority of drain-source potential, V_{ds} [6]. This interpretation is confirmed by the deduced I_d values regrouped in Table 2 for both types of MESFETs. Therefore, the linear decrease of the curves of Fig. 6 could

be due to a decrease of drain current caused by increasing of $|V_{gs}|$.

Table 2. Drain current variation with gate-source voltage for both GaAs MESFETs.

$-V_{gs}$ (V)	$I_d]_{MESFET-1}$ (mA)	$I_d]_{MESFET-2}$ (mA)
0.20	23	16.4
0.30	15	9.23
0.35	11.5	7.3
0.40	5.7	4.68
0.45	1.1	3.01
0.60	0.2	0.29

3. Conclusions

The output conductance variation with frequency was investigated for commercial GaAs MESFETs. The present methodology is based on the comparison of theoretical and experimental results to identify the internal operating temperature from the best curves agreement. A positive dispersion was found that for low frequencies ($f \leq 4\ 10^3$ Hz) whereas for high frequencies, $|g_d(f)/g_d(lf)|$ values become constant for all values of V_{gs}. The agreement between calculated and experimental results is obtained at a very precise temperature with is considered to be the device operating temperature. This temperature was found to decrease linearly with V_{gs}: an increase of $|V_{gs}|$ introduces a decrease in this temperature according to a law that was found to be: $T(K) = T_0 - \beta V_{gs}$. This relation puts into evidence the close relation between bias conditions of the GaAs MESFET and its degree of self heating.

References

[1] J. Jyegal, Appl. Phy. **111,** 054513 (2012).

[2] J. Golio, M. Miller, G. Maracas, D. Johnson, IEEE Trans. Electron Devices **37,** 1217 **(**1990**).**

[3] J. Graffeuil, Z. Hadjoub, J. P. Fortea, M. Pouysegur, IEEE Solid State Electronics **29,** 1087 (1986).

[4] A. Raffo, V. Vadalà, P.A. Traverso, A. Santarelli, G. Vannini, F. Filicori, Computer Standards & Interfaces **33,** 165 (2011).

[5] W. Liu, Il-Y. Chung, L. Liu, S. Leng, D. A.Cartes, Engineering Applications of Artificial Intelligence **24,** 132 (2011).

[6] P. C. Canfield, S. C. F. Lam, D. J. Allstot, IEEE Solid State Circuits **25,** 299 (1990).

[7] Y. Hasumi, N. Matsunaga, T. Oshima, H. Kodera, IEEE Trans. Electron. Devices **50,** 2032 (2003).

[8] Z. Hadjoub, K. Cheikh, A. Doghmane, Optoelectron. Adv. Mater. -Rapid Commun. **3,** 360 (2009).

[9] A. Khoualdia Z. Hadjoub, A. Doghmane, Int. J. Nanoelectronics and materials **3,** 9 (2010).

[10] S. H. Wemple, H. Huang, in GaAs FET Principles and Technology, J. V. Dilorennzo D. D. Khandelwac, Eds. Dedham, MA: Artech House, 1982, p. 313.

[11] G. A. Umana-Membreno, J. M. Dell, B. D. Nener, L. Faraone, G. Parish, Y.-F. Wu, U. K. Mishra, IEEE Conference, 1999, p. 252.

[12] G. Meneghesso, A. Paccagnella, Y. Haddab, C. Canali, E. Zanoni, Apply Phys Lett **69**, 1411 (1996).

[13] J. Lagowski, D.G. Lin, T. Aoyama, H. C. Gatos, Proc.3rd semi-insulating III-V materials conf. (Kah-nee-ta,OR), D. C. Look and J. S. Blakemore, Eds. Natwich, UK Shiva, 1984, p.222.

*Corresponding author: a_doghmane@yahoo.fr